Enhanced flood risk with 1.5 °C global warming in the Ganges–Brahmaputra–Meghna basin

Environmental Research Letters

LETTER

Enhanced flood risk with 1.5 °C global warming in the Ganges–Brahmaputra–Meghna basin

P F Uhe[1], D M Mitchell[1], P D Bates[1], C C Sampson[2], A M Smith[2] and A S Islam[3]

[1] School of Geographical Sciences, University of Bristol, United Kingdom
[2] Fathom, Engine Shed, Station Approach, Bristol, United Kingdom
[3] Institute of Water and Flood Management, Bangladesh University of Engineering and Technology, Dhaka, Bangladesh

E-mail: Peter.Uhe@bristol.ac.uk

Keywords: flooding, climate change, Ganges–Brahmaputra–Meghna, 1.5°C global warming

Supplementary material for this article is available online

OPEN ACCESS

RECEIVED
26 March 2018

REVISED
13 March 2019

ACCEPTED FOR PUBLICATION
19 March 2019

PUBLISHED
16 July 2019

Abstract

Flood hazard is a global problem, but regions such as south Asia, where people's livelihoods are highly dependent on water resources, can be affected disproportionally. The 2017 monsoon flooding in the Ganges–Brahmaputra–Meghna (GBM) basin, with record river levels observed, resulted in ~1200 deaths, and dramatic loss of crops and infrastructure. The recent Paris Agreement called for research into impacts avoided by stabilizing climate at 1.5 °C over 2 °C global warming above pre-industrial conditions. Climate model scenarios representing these warming levels were combined with a high-resolution flood hazard model over the GBM region. The simulations of 1.5 °C and 2 °C warming indicate an increase in extreme precipitation and corresponding flood hazard over the GBM basin compared to the current climate. So, for example, even with global warming limited to 1.5 °C, for extreme precipitation events such as the south Asian crisis in 2017 there is a detectable increase in the likelihood in flooding. The additional ~0.6 °C warming needed to take us from current climate to 1.5 °C highlights the changed flood risk even with low levels of warming.

1. Introduction

In many regions around the globe, climate change is increasing the severity of damaging flooding events [1–4]. Flooding in large rivers such as the Ganges–Brahmaputra–Meghna (GBM) system can affect millions of people through damage to property, crops and livestock and risks to life. Globally, climate change is expected to result in more rainfall, due to the ability of a warmer atmosphere to hold more water [5]. However, changes to local and regional rainfall are also impacted by a number of factors such as topography, atmospheric composition (e.g. aerosols) [6, 7], land-use change [8], ocean currents and atmospheric circulation. So when evaluating the risk of severe storms and flooding, it is critical to look at changes on regional scales.

The recent United Nations Framework Convention of Climate Change agreement in Paris has committed to restricting warming levels to well below 2 °C and aiming for 1.5 °C above pre-industrial levels [9]. There has recently been a concerted effort to run climate simulations designed to inform us of the impacts of 1.5 °C and 2 °C warming. Two initiatives have designed climate simulations to represent 1.5 °C and 2 °C of global warming: (1) the Half a degree Additional warming, Prognosis and Projected Impacts (HAPPI) project [10], includes many atmospheric-only simulations using super-ensembles (>100) and multiple models to give a range of possible climate responses. (2) The 'CESM Low Warming' project [11], uses a single coupled atmosphere-ocean model to achieve climates stabilized at 1.5 °C or 2 °C of global warming, thereby providing a more complete sample of ocean variability than HAPPI, but at the expense of smaller sample sizes. These simulations give decision makers more targeted information than more general initiatives, about the benefits of restricting the level of global warming [12].

This study investigates flooding in the GBM river system which covers a wide area, through Bangladesh, Bhutan, China, India and Nepal. Rainfall over the

GBM system is dominated by the monsoon season (June–September). Around 80% of Bangladesh is floodplain, with floods affecting tens of millions of people occurring every six years or so [13]. Any amplification of flood hazard may have grave implications for the vulnerable and exposed populations in these regions. Previous studies for the GBM have predicted increases in future peak river discharge [14–18] and flood extent [19]. Recent studies [3, 20–22], looked at flood risk at 1.5 °C and 2 °C of global warming, for changes to peak discharge of the Brahmaputra or global flood risk including the Ganges–Brahmaputra. However, these used high emissions scenarios to determine 1.5 °C and 2 °C of global warming.

The precipitation response for a given level of warming can differ between low and high emissions scenarios [12] and between transient and stabilized climates. It has been found that short duration extreme rainfall is constrained by the amount of global warming [23], however this may vary due to aerosols in areas with high levels of pollution [24]. Additionally, in the GBM, we consider longer duration extremes which not may be as directly constrained by temperature. The targeted low warming scenarios are designed to represent a stabilized climate, and avoid complications introduced by determining specific warming levels from transient simulations rising to higher levels of warming. The low warming scenarios also have lower aerosol levels than present day [25], as projected for the end of the 21st century. These aerosol levels will differ significantly from those in time slices at 1.5 °C and 2 °C, from high emissions scenarios, as these will occur earlier in the 21st century. So results from these experimental designs will differ where aerosols play an important role.

Determining flood impacts requires a nonlinear transformation of river discharge using a hydrodynamic model because the floodplain topography and channel-floodplain hydraulic interactions included in such schemes may either amplify or dampen the flooding response to changing discharge. We therefore extend previous studies by analyzing flood inundation using a high-resolution hydraulic model to represent the possible change in flood risk, based on these low warming scenarios.

2. Methods and datasets

2.1. HAPPI atmospheric simulations

Simulations were used from the HAPPI project: atmosphere-only climate simulations, forced by sea-surface temperatures (SSTs), sea-ice concentration (SIC) and green-house gas concentrations. SSTs and SIC were from the OSTIA observational dataset [26] for current day (Hist) simulations (2006–2015), and SSTs from the Coupled Model Intercomparison Project Phase 5 (CMIP5 [27]) output were used to estimate the future scenarios corresponding to 1.5 °C and 2 °C global warming above pre-industrial conditions, at the end of the 21st century [10]. Large ensembles were produced by running simulations with different initial condition perturbations. Seven models were used for this analysis (table S2), and most of the models had around 100 simulations or more for each of the scenarios (table S3).

2.2. CESM-CAM5 low warming simulations

Simulations using the CESM-CAM5 coupled climate model were designed using specific GHG concentration pathways, to stabilize temperatures at 1.5 °C and 2 °C global warming above pre-industrial conditions by 2100 [11]. These simulations cover 2006–2100, and are continuation runs of 11 CESM-CAM5 historical simulations (1920–2005) [28] run as per the CMIP5 design [27]. For current day climate, the 2006–2015 decade from the 2 °C simulations was analyzed, to match the time period of the HAPPI current day simulations. The 2090–2099 decade was analyzed for the future scenarios.

2.3. Climate data analysis

Area averages over the GBM river basin were calculated from climate model outputs. The basin definitions were identified based on the HydroBasins dataset [29]. For each model, years from different ensemble members were pooled for analysis, resulting in a large number of years representing the historical, 1.5 °C and 2 °C worlds in each model (10 years per simulation multiplied by number of ensemble members as per table S3). Values such as ensemble means were calculated across the distributions of years and ensemble members. Observational datasets were used for model evaluation (see table S4).

We primarily analyzed the yearly maximum of monthly rainfall (RXmonthly). This is because the characteristic duration of rainfall event resulting in the largest flooding events in the GBM is on the order of a month or longer, so this variable was chosen as a proxy for the change in river discharge in the GBM (see section 2.5). We also looked at yearly average precipitation and yearly maximum of 5 day mean rainfall (RXx5day), which is a standard climate change index defined by the Expert Team on Climate Change Detection and Indices [30, 31]. RXx5day represents extreme rainfall connected to flooding in small catchments or tributaries. We validated the seasonal cycle of precipitation and monsoon winds in the region for each of the models.

The climate models have precipitation biases, (compare 'OBS/Reanalysis' with 'Hist' in figures 1(a) and (b)), with the majority of models over-predicting the peak rainfall. Some of the models also tend to simulate an early monsoon onset compared to observed (figure 2). We additionally note that the observational datasets have limitations. There are differences between precipitation observation datasets

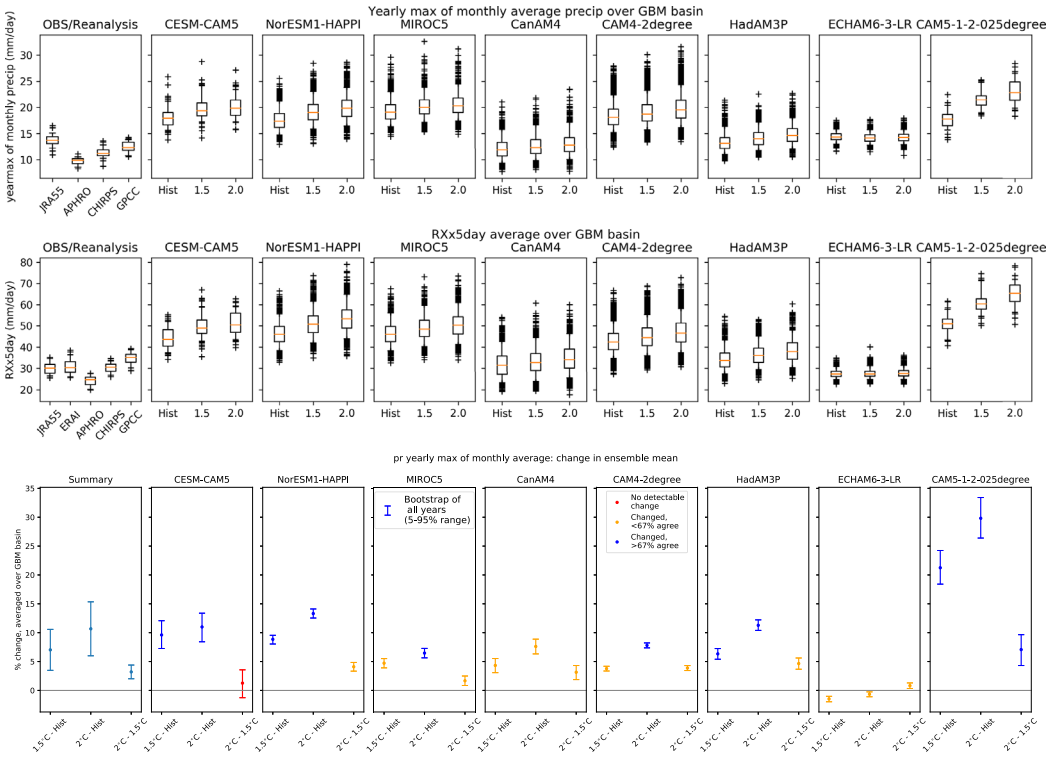

Figure 1. Distributions of precipitation averaged over the GBM basin. (a) Shows boxplots of RXmonthly for each of the models and also observations. (b) as per (a), but showing RXx5day, (c) percentage changes in ensemble mean RXmonthly, between the different scenarios '1.5 °C—Hist', '2 °C—Hist', and '2 °C–1.5 °C'. Error bars show the 5%–95% range of sampling uncertainty in the ensemble mean change, based on randomly resampling each distribution 1000 times. Color indicates additional measures of significance: Red symbols indicate the distributions of simulated years are not distinguishable between the two scenarios compared, based on a two sided Kolmogorov–Smirnov test at $p = 0.05$. For the other colors, there is a detectable difference between the distributions. Additionally, blue and yellow symbols give an idea of the magnitude of change relative to year-to-year variability. Blue or yellow symbols indicate whether the proportion of ensemble members which change in the same direction as the mean is greater or less than 67%. The first panel of (c) shows the multi-model summary which does not used color to indicate significance. OBS/ Reanalysis datasets are defined in table S4.

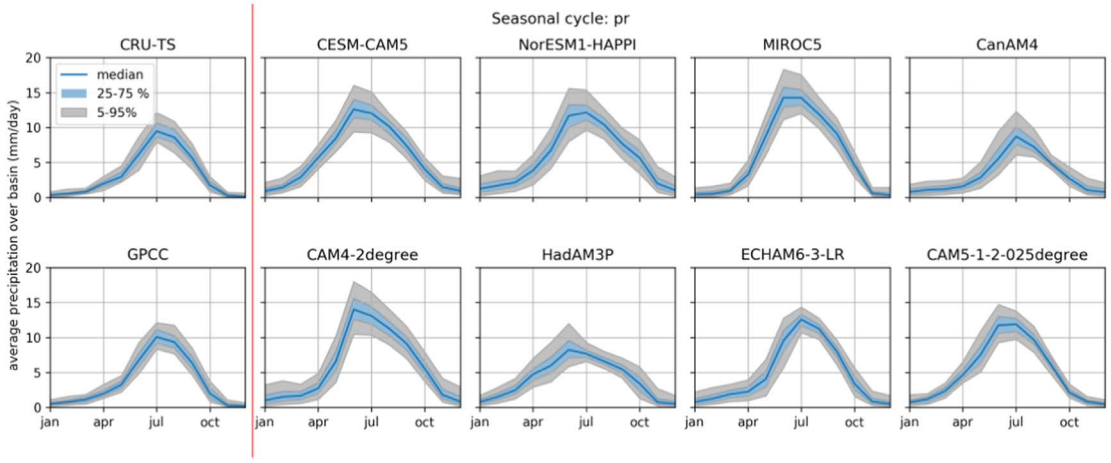

Figure 2. Seasonal cycle of precipitation averaged over the GBM basin. Each model is shown in a separate panel. Two observational products (CRU-TS and GPCC), defined in table S4, are shown in the left-most panels.

(figures 1(a) and (b)), and it has also been suggested that high-altitude precipitation (such as over the Himalayas), may be significantly underestimated in observations, due to poor coverage of stations and underestimation of solid precipitation [32, 33].

Our projection of future changes in flooding is based on precipitation changes in the climate models, rather than the absolute conditions in those models. The response of precipitation to climate change predicted by the models is based on physical mechanisms,

which may represent the relative increase or decrease in precipitation even in the presence of biases. We concentrate our analysis on the basin scale, to reduce the influence of small scale effects, which the models have difficulty representing. Bias-correction, can be applied to remove biases in the mean (and variability), but should leave the relative change in precipitation unchanged. However, this is not always the case for changes in extremes [34], so bias-correction methods need to be applied with caution. We analyze scaling factors based on the relative change in precipitation, and do not apply bias correction for this study.

As the Asian monsoon drives the majority of precipitation over the GBM region, it is important that the climate models represent the monsoon circulation. Separate analysis including most of the HAPPI models used here has been made for the Asian monsoon precipitation [35, 36] and specifically for monsoon onset and length [37]. These studies determined that the HAPPI models capture the Asian monsoon circulation sufficiently to investigate future changes in precipitation. Reference [35] showed an increase in both intensity and frequency of extreme precipitation in the region, and increases in particularly damaging persistent rainfall extremes in northern India. An evaluation of the large scale 850hPa winds for each model, and its change between scenarios, is shown in figure 3. The models have varying biases in the monsoon winds, although MIROC5, with the highest precipitation, has a notable strengthening of the monsoon winds relative to the ERA-Interim reanalysis. The patterns of change in the monsoon circulation vary between between 1.5 °C—'Hist', and 2 °C–1.5 °C, and vary between models, which is consistent with [36], who additionally concludes that the precipitation change is dominated by the thermodynamic response and changes related to circulation are more uncertain.

2.4. Flood hazard model simulations

Flood hazard was estimated by the use of the Bristol global flood model [38]. In this modeling framework, calculations of flood extent are performed with an implementation of the well-known LISFLOOD-FP flood inundation model [39]. LISFLOOD-FP is a hydraulic model, solving the 2-dimensional shallow water equations. This configuration of the model uses a recently published bare-earth version of the Shuttle Radar Topography Mission (SRTM) global elevation database (MERIT DEM [40]), and global river and catchment hydrography from HydroSHEDS [29] to determine catchment areas and channel locations. It applies a Regional Flood Frequency Analyses (FFA) [41] using global data for river discharge (Global Runoff Data Centre (GRDC) dataset) and rainfall. In this approach, river hydrographs for locations not included in the GRDC dataset were estimated based on distributions from rivers with similar characteristics. For this study, the FFA based on global data was adjusted using gauge data from the Ganges and Brahmaputra rivers to represent the local discharge more accurately.

A limitation of the MERIT DEM used by the hydraulic model, is that it does not include flood defenses. For example the western banks of the Brahmaputra are protected by embankments from Chilmari to Sirajganj, so flood extents simulated by the model will differ with observations in these areas.

This model has previously undergone extensive validation for catchments in the UK and Canada [38], and in the USA [42]. They found that the model performance approaches the skill expected by models built with high quality local data, and that the model performs better for wet regions and rivers with larger catchments [42]. The improved MERIT DEM dataset used in this study may also improve the model performance (compared to SRTM topography used in [38] and [42]). We evaluate the performance of the model along a stretch of the Brahmaputra river in section 3.2.

For this paper, new simulations were performed over the region 21–31N, 84–94E. The hydraulic model simulated flood inundation at 30 arc second (~900 m at the equator) resolution, which was downscaled to the MERIT DEM at 3 arc second resolution. The model simulates fluvial flooding in catchments above ~50 km^2. For this study, flood hazard for return periods of 1 in 5, 1 in 20 and 1 in 100 years were calculated. This covers a large portion of the GBM basin, including the whole of Bangladesh. Firstly a 'baseline' simulation was calculated using observed distributions of current river discharge and rainfall, and secondly simulations were run with scaled river discharge to represent changes due to global warming. Changes in flood area and flood depth, between the baseline and future scenarios, were analyzed over the region and additionally over the sub-basins Ganges, Brahmaputra and Meghna (regions shown in figure S1 is available online at stacks.iop.org/ERL/14/074031/mmedia).

2.5. Scaling discharge from future scenarios

To determine scaling factors based on the global warming scenarios, the change in RXmonthly was used as a proxy for the change in river discharge. This was chosen as we are interested in the peak flows, and in the GBM system the highest flood waters due to the monsoon rains build up over a period of at least a month. This metric represents the change in precipitation driving flooding events, however we note that this does not take into account, evaporation or catchment hydrology, which may cause discharge to scale differently to the change in precipitation. This may also vary by return period, for example table 3 in [20], however these numbers have large uncertainty ranges (e.g. figure 5 in [22]). Furthermore, a comparison of precipitation and runoff for models used in this study, show consistent changes between these two variables (figure S3). As discharge results from the accumulation of runoff, this gives us confidence in our proxy as an

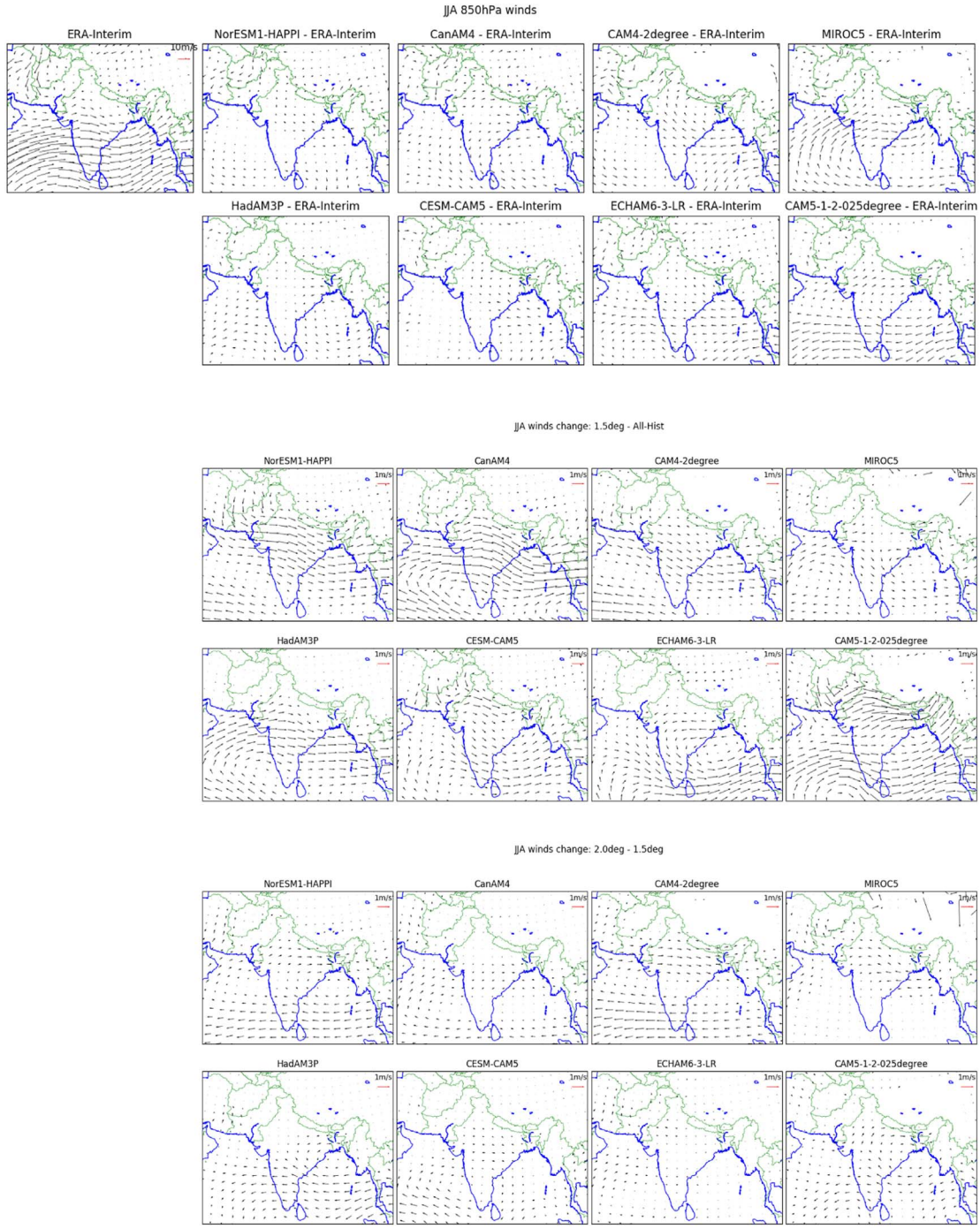

Figure 3. Figures showing JJA average 850 hPa winds. (a) ERA-Interim winds and differences between each model and ERA-Interim for 2006–2015 period. (b) Difference between 1.5 °C and 'Hist' scenarios for each model. (c) Difference between 2 °C and 1.5 °C for each model. All data was interpolated to a common 2° horizontal resolution grid before plotting.

approximation of future change. The advantage of this simple approach is that it does not rely on potentially problematic bias correction methods, or hydrological modeling that may be under-constrained due to sparse observations and hence introduce a greater level of uncertainty.

We determined the percentage change in RXmonthly, between the current day climate and 1.5 °C and 2 °C worlds, averaged over the GBM basin. The ensemble mean was calculated separately for each of the 8 models considered (7 HAPPI models and CESM). A weighted average taking into account the sampling uncertainty and model spread was used to produce a best estimate (referred to as the Multi-Model Summary, see text S3). The best estimates were 7.0% ± 3.6% and 10.7% ± 4.7%. The best (medium) estimates along with the upper (high) and lower bound were used to scale the baseline/present day precipitation and river discharge in the hydraulic model for the future scenarios.

3. The 2017 flooding event in the GBM basin

High rainfall in the monsoon season in South Asia caused particularly severe flooding in 2017. This flooding was reported in the media to have killed over 1200 people in India, Nepal and Bangladesh, and millions were evacuated or otherwise affected [43, 44]. In Bangladesh, reports indicated that over 6.1 million people were affected with a death toll of at least 134 [43, 45]. The high impact of this event makes it a relevant case study to evaluate the skill of the hydraulic model in simulating inundation extent from a recent event. The following section describes the peak level of the Brahmaputra river in August 2017, and a comparison showing the skill of modeled inundation extent against satellite observations.

3.1. Peak river level measured at Bahadurabad

On the 16th of August, the Brahmaputra recorded a record high level of 20.84 m at Bahadurabad. However, an analysis of river discharge at this station shows that despite being a record river level for this particular gauging site, the discharge for this event (78 500 $m^3 s^{-1}$, measured on the 17th of August) was only a 1 in 5 year return period flow (95% confidence interval 3–9 years).

Other than the uncertainty in discharge measurements, the discrepancy between the return periods for river level and discharge at Bahadurabad is most likely explained by very local changes in the river channels from sedimentation and construction of flood embankments. The relationship between discharge and river height is a local effect around the gauge as a result of erosion and deposition as mobile sediment waves move through the system. However at the reach scale that we consider here these local variations will cancel out and our overall estimates of the impact of increasing flows on inundation extent will be reasonable ones. The discharge return period for this event is used for the following comparison, as discharge is used to drive the hydraulic model.

3.2. Representation of 2017 event in the flood hazard model

Because ground based measurements of flood extent do not exist at the resolution of the flood model, we compared flood extent from the model with estimates from two satellite products: (1) Copernicus Sentinel-1 Synthetic Aperture Radar (SAR) data and (2) the Joint Research Centre Global Surface Water (GSW) dataset [46], which is produced from Landsat imagery. The Sentinel data at ~10 m resolution was processed and water bodies were detected based on the backscatter amplitude (supplementary text S1). SAR products can penetrate clouds, so the Sentinel-1 data can give a snapshot of inundation extent. The GSW dataset provides a flood recurrence product at ~25 m, based on many images over the 1984–2015 period.

The 1 in 5 year modeled hazard was compared over a region downstream of the Bahadurabad gauge (89–90E 24.4–25.2N, figure S2). We compared this against a single Sentinel-1 image from 22 August 2017. This is not exactly like-for-like, as the flood model uses a 1 in 5 year discharge everywhere, whereas the actual flow in different river segments will be greater or lower depending on local conditions. We also compared against flood recurrence greater than 20% (5 years) in the GSW dataset.

Detection of flood extent in satellite data is not exact, both false positives and missed detection are possible. For example, in SAR data, smooth surfaces such as roads or mud flats may in some cases be classified as water, water roughened by wind may be classified as land, and flooded areas covered by vegetation may not be detected due to backscatter effects. Topographical shadow effects may cause false positives as well. Some of these effects, such as topographical shadows, can be corrected by the image processing, but this is still not a perfect representation of the ground situation. The GSW dataset will also not detect bodies of water obscured by vegetation, and persistent cloud cover may cause short duration flooding events to be missed.

Figures 4(a)–(b) compares model flooded regions with satellite data, at the satellite's resolution. The flood model captures a large proportion of the complicated braided river structure and flood plain. Figure 4(a) shows the modeled fluvial flood extent against the Sentinel data for 2017. As only ~7% of the catchment areas reside in Bangladesh, we expect the fluvial flooding to drive the majority of the flooding. On the flood plain to the east of the river, the modeled fluvial flooding under-predicts the Sentinel flood extent (figure 4(a)). Figure 4(b) shows the modeled fluvial flooding against the GSW flooding. The model shows better agreement with the GSW dataset than the Sentinel image. This may be either to do with the nature of the different instrumentation and processing picking up different types of flooding or because the the GSW data is a recurrence product which more closely represents the 1 in 5 year maximum extent as the model does, compared to the Sentinel data which is a snapshot of flooding on 22 August 2017.

In the region to the west of the river, the model is over-predicting the observed event. This is probably because the western bank of the Brahmaputra river is protected by an embankment that is not represented in the MERIT DEM and therefore not in the model. In addition, the hydraulic model simulates a 1 in 5 discharge in all river segments in the domain, so this comparison is less valid in other parts of our domain which may have a different return period for 2017.

Metrics representing this comparison were calculated over this region. Using the Critical Success Index (see [42], supplementary text S2) the model fluvial

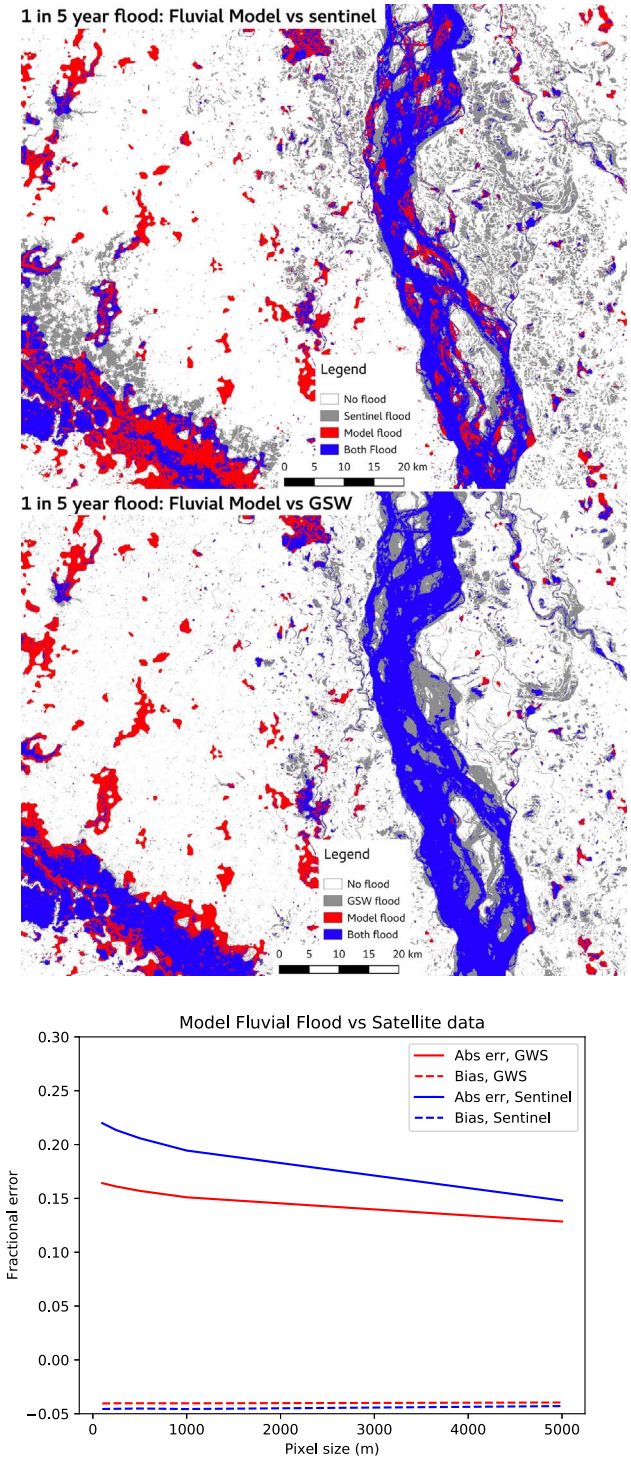

Figure 4. Satellite data versus model: (a) comparison of model 1 in 5 year fluvial flooding versus Sentinel flooding from 22 August 2017. (b) Comparison of 1 in 5 year flood extent, model fluvial flooding versus GSW. (c) Absolute fractional error and bias between model and satellite flood areas aggregated to different scales.

flood extent has a score of 0.47 for GSW and 0.36 for Sentinel. This shows lower performance than shown in [42] and [38]. As matching the higher resolution satellite data is a very difficult test we also calculated the absolute fractional error between data aggregated to larger scales (figure 4(d)), with errors of 0.22 (Sentinel) and 0.16 (GSW) at 100 m, reducing to 0.13 and 0.15 respectively at 5 km.

Given this $<$ 15% error in fractional flooded area at 5 km, we conclude that the model is fit for the the sub-basin scale relative change analysis which we perform here. The hydraulic model is a physically based model, and is mass and momentum conserving. So the evaluation of the 1 in 5 year event gives us confidence that the relevant physics and the topography is well represented by the model and a greater return period

of river flow will result in a realistic flood inundation for the 1 in 20 and 1 in 100 year events.

4. Changes in flood risk at 1.5 °C and 2 °C warming

4.1. Simulated mean and extreme precipitation in the GBM

Changes to GBM precipitation are shown for RXmonthly in figure 1(c). All except for one of the models shows a wetter climate in the future scenarios, and in the 2 °C simulations, greater than two-thirds of years are wetter than the mean in the current climate, for all except two of the models. ECHAM6-3-LR shows a small drying to 1.5 °C, but an increase between 1.5 °C and 2 °C. Similar but slightly higher changes are seen for RXx5day (figure S4) and lower changes for yearly precipitation (figure S5), showing a greater wetting change for shorter duration events. Figure 1(c) gives estimates for the ensemble mean change, which in general may differ from the changes of higher return period events. However, in this study, changes for different return periods are consistent within the sampling uncertainty and there is no systematic trend of higher or lower scaling of precipitation at higher return periods (figure S6). We additionally note that using the ensemble mean may result in underestimating the uncertainty as the sampling uncertainty increases for higher return periods.

In all of the models apart from CAM4-2degree, the 1.5 °C—'Hist' change is greater than the 2 °C–1.5 °C change. This is partly because the global warming from historical to 1.5 °C is greater (~0.6 °C) than between 1.5 °C and 2 °C (0.5 °C). Comparing the RXmonthly change per degree of warming (figure S7), half of the models still show a greater change for 1.5 °C —'Hist', however the other models show no-change or a smaller change, so there are nonlinear changes between scenarios which vary between the models. These differences may be due to the removal of suppressive effect of rainfall between 'Hist' and 1.5 °C, and varying representations of aerosols in the model. The patterns of circulation changes also differ between 1.5 °C—'Hist' and 2 °C–1.5 °C in all of the models (figure 3), so different mechanisms may be dominating in the different models.

4.2. Changes in flooding

Flood hazard maps were produced using the hydraulic model for the baseline period and low, medium and high estimates for the 1.5 °C and 2 °C scenarios. The changes in flooded area over the region are shown in figures 5(a) and (b) for the medium estimate of the 1.5 °C scenario for 1 in 5 and 1 in 100 year flood hazards. A zoomed in section shows the area around Dhaka. The 1 in 5 year hazard has a much smaller flood extent than the 1 in 100 year hazard, but crucially the change in additional area flooded between 1.5 °C and the baseline (red regions) is considerably larger for the 1 in 5 year hazard than the 1 in 100 year hazard, highlighting the importance of changes in these frequently occurring events. The changes to the depth of flood waters for the same simulations are shown in figure 5(c) and (d) with large areas increasing flood depth by 20 cm and smaller areas increasing by 50 cm or more. The medium 2 °C scenario shows incrementally larger changes compared to the 1.5 °C scenario, in both flood area and flood depth (figure S8).

The changes in flood extent were aggregated over three sub-regions representing the Ganges, Brahmaputra and Meghna basins. These are shown in figure 6 for each of the scenarios and 1 in 5, 1 in 20 and 1 in 100 year flood hazard. The more frequent (less severe) flood hazards, show greater percentage increases in flood extent than the more extreme flooding events. This may be expected by the nature of river valleys as lower, flatter areas will flood in the less severe events. However, when the flood waters reach steeper areas in more extreme events, the relative increase in area will be less for a given change in water level. The relative change in the 1 in 5 year flood area (figure 6, blue and red bars) is greater than the corresponding relative precipitation change (blue and red shading). There are small differences between the basins, but the relative change in flood area consistently decreases for the 1 in 20 and 1 in 100 year floods. The 1 in 100 year flood area in the Ganges and Brahmaputra rivers show a smaller change than the relative precipitation change.

Figure 6 shows the percentage area *relative* to the baseline flood increase, however the *absolute* change in area does not show a consistent trend with the return period of the event (figure S9). We also note that the 1 in 100 year events experience a greater change in flood depth, so these particularly extreme events may become more destructive due to higher flood waters, even without the flooded area increasing dramatically.

5. Discussion

The Paris Agreement calls to restrict global warming to well below 2 °C and aim for 1.5 °C. The simulations used here reflect those goals and may give different results to evaluating 1.5 °C and 2 °C in high emission scenarios such as used for CMIP5. The climate models employed here show a significant trend of increasing rainfall in the GBM for all except one of the models analyzed. This trend is stronger for extreme rainfall than average rainfall which has implications for flooding. Even at a low level of global warming of 1.5 °C, the wetting signal in the GBM is clear, and given it is proximity to densely populated regions, this translates to increased flood risk. There is also a statistically significant increase in monsoon precipitation between 1.5 °C and 2 °C despite there being overlap in the uncertainty ranges of changes from present day to 1.5 °C and 2 °C (figure 1(c)). This shows there is a clear

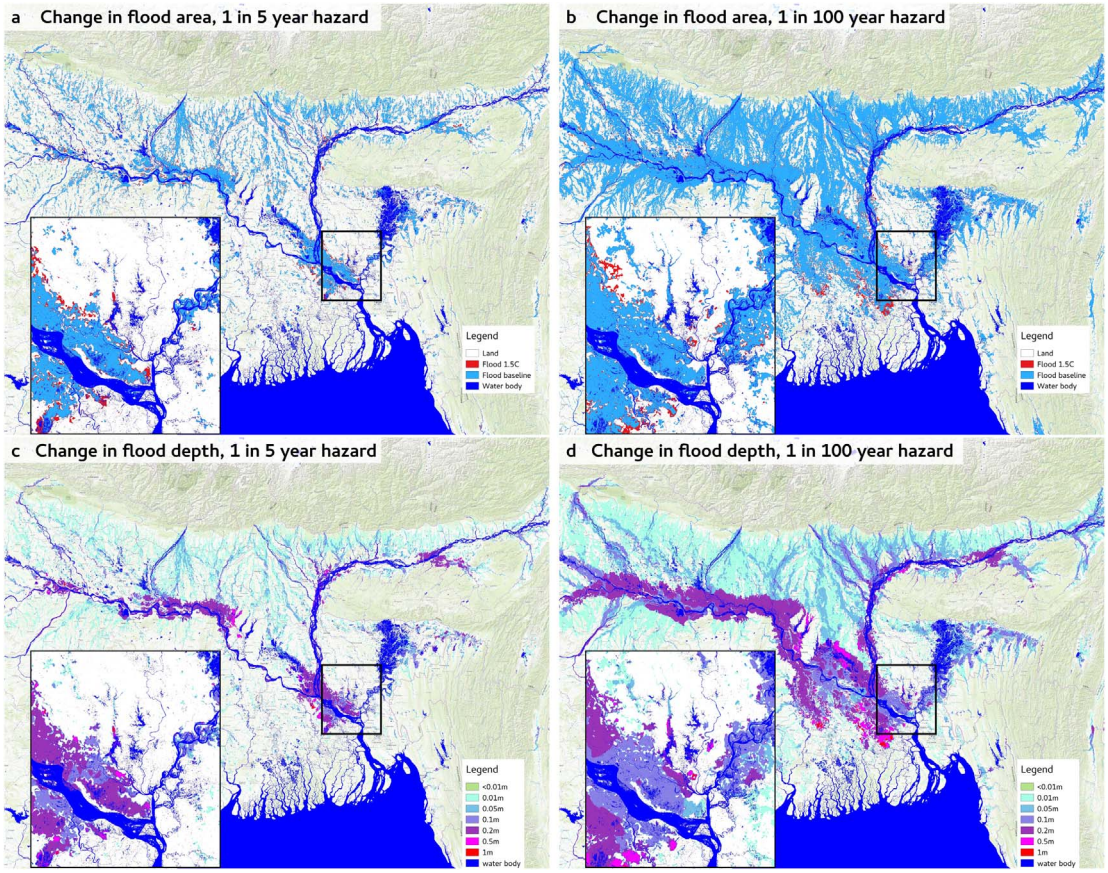

Figure 5. Simulated changes in flood extent and depth between 1.5 °C and the baseline. (a) and (b) Change in flood extent due to fluvial flow, for 1 in 5 year and 1 in 100 year hazards respectively. Regions are separated into 'Land' (not flooded), 'Flooded baseline' and 'Flooded 1.5 °C' (additional areas of flooding), and 'Water body' (permanent water). (c) and (d) Change in flood depth due to fluvial flow, for 1 in 5 and 1 in 100 year hazards respectively. All panels show the change in the 'medium' 1.5 °C scenario compared to the baseline simulation.

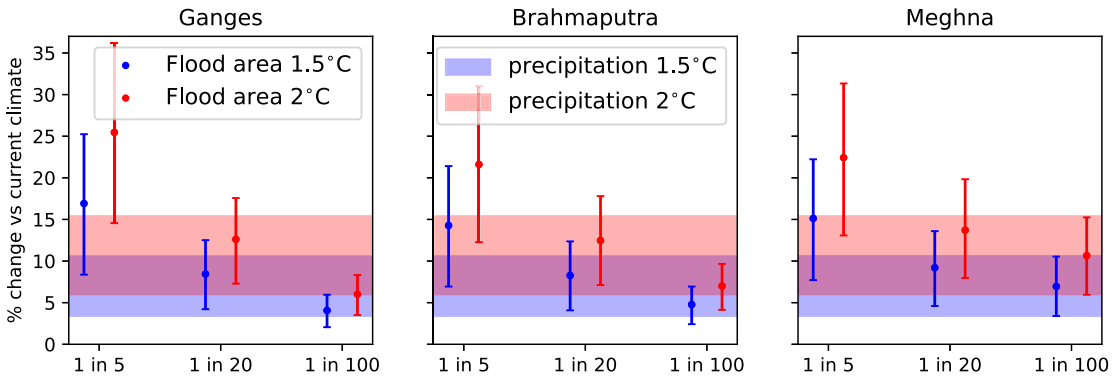

Figure 6. Aggregated changes in flooded area for three sub-basins. Changes in flooded area relative to baseline flooded area for each scenario, for 1 in 5, 1 in 20 and 1 in 100 year flood hazard. Changes are shown over the three sub-basins Ganges, Brahmaputra and Meghna (figure S1). The medium estimate is shown as a dot; low and high estimates are shown by the extent of the error bars. The shaded area marks the range in percentage change in precipitation between the low and high estimates for the 1.5 °C (blue) and 2 °C (red) scenarios.

benefit in reducing flood risk by keeping temperatures to the lower target.

The precipitation change between current climate and 1.5 °C is greater than the change between 1.5 °C and 2 °C. However, due to experimental design, less of the models show this trend for change in precipitation per degree of warming. The design of the low warming experiments also results in greater aerosol change between Hist and future climates, than between 1.5 °C and 2 °C, which may not be the case in high emission scenarios.

In addition to aerosol influence, there may be non-linear changes in the monsoon circulation in this region, which are uncertain based on climate model

projections (see figure 3 and [36]). The model mean signal in precipitation may be dominated by the thermodynamic response, with differences between models due to the representation of changes in the monsoon.

There are advantages and limitations in different modeling setups. Coupled atmosphere-ocean models (e.g. CESM-CAM5) sample a wide range of possible ocean variability, and atmosphere only models (e.g. HAPPI) may underestimate this variability [47]. However the use of prescribed SSTs also reduces problematic biases present in coupled models [48]. In this study, having consistent projections from both type of models gives us greater confidence that our conclusions are not skewed by the choice of experimental design.

Increased river flow is expected to have a more noticeable impact on the flood extent for less extreme events. This nonlinear response of the flood area to the change in river flow highlights the importance of the floodplain topography. Modeling only the change in precipitation or river discharge may therefore be misleading. Using a hydraulic model to map inundation extent is needed to convey the full impacts of climate change on floods.

This study applies a scaling factor to river discharge based on the modeled changes in precipitation. This is a simplification assuming the leading order effects related to flood hazard are from the direct precipitation response. It also assumes that the shape of distributions of discharge do not change with global warming, which would change the relative magnitudes of floods at different return periods. However, any changes in the shape of the distribution are highly uncertain and are not supported by our climate simulations (figure S6). This approach also does not take into account all of the catchment hydrology that contributes to river flow and there are there are influences from changes in temperature, glacial melt and rainfall-runoff processes. However, we find that that for the subset of climate models where runoff is calculated, the runoff scales very similarly to precipitation (figure S3). There are also uncertainties modeling river flow, especially in data sparse regions such as the GBM. So this approach avoids introducing additional uncertainty and complexity, with the caveat that we are attributing changes in flood risk to changes in precipitation only and not other catchment effects. In addition, the use of RXmonthly for our proxy is most relevant to the downstream river sections as flooding in upstream catchments will have a faster response time. Our analysis showed that for shorter events (e.g. RXx5day), the climate change influence is stronger, so RXmonthly is a conservative choice.

Another significant contributor to river flow in this region is glacier melt. In the upper sections of the Ganges and Brahmaputra, glacial melt contributes about 11% and 16% of average runoff respectively (see table S7 in [49]). For the Upper Brahmaputra, this increases to around 20%–25% during months of peak flow (figure S6 in [49]). In the near future, glacier melt may have a small increase (scenario dependent), however after 2040–2050, glacier melt is projected to decline [49–52]. This is a result of a balance between increased melting rates at warmer temperature and reduced glacier mass. Following this, in the scenarios stabilized at 1.5 °C or 2 °C around the end of the 21st century, the contribution of glacier melt to river flow would be expected to be slightly reduced compared to present day.

The population in South Asia is highly reliant on water resources for subsistence agriculture, and is strongly impacted by floods. We show a clear anthropogenic signal in precipitation change in the GBM basin and a subsequent response in flood area at 1.5 °C and 2 °C warming. The relative change in flood extent varies with event intensity which is important to note for adaptation measures. This study shows the use of precipitation changes to scale river discharge is a justifiable approximation to gauge the sensitivity of flood hazard. For future studies, it will be important to investigate a wide range of river systems in depth to see what, if any, change is discernible due to climate change, even with high levels of mitigation.

Acknowledgments

This research used science gateway resources of the National Energy Research Scientific Computing Center, a DOE Office of Science User Facility supported by the Office of Science of the US Department of Energy under Contract No. DE-AC02-05CH11231. HAPPI core support was part funded by Google DeepMind. DM is supported by a NERC Research Fellowship. PB is supported by a Leverhulme Research Fellowship and a Royal Society Wolfson Research Merit Award. ASI is supported by a Oxford Martin School Fellowship. The HAPPI project data is freely available. See http://happimip.org/happi_data/ for details. CESM Low Warming simulations are freely available here: https://doi.org/10.5065/D6RV0MD6. Code for analysis and the flood model output can be made available on request to corresponding author.

ORCID iDs

P F Uhe https://orcid.org/0000-0003-4644-8559
D M Mitchell https://orcid.org/0000-0002-0117-3486
P D Bates https://orcid.org/0000-0001-9192-9963
A S Islam https://orcid.org/0000-0002-2435-8280

References

[1] Pall P, Aina T, Stone D A, Stott P A, Nozawa T, Hilberts A G J, Lohmann D and Allen M R 2011 Anthropogenic greenhouse gas contribution to flood risk in England and Wales in autumn 2000 *Nature* **470** 382–7

[2] Schaller N *et al* 2016 Human influence on climate in the 2014 southern England winter floods and their impacts *Nat. Clim. Change* **6** 627–34

[3] Alfieri L, Bisselink B, Dottori F, Naumann G, de Roo A, Salamon P, Wyser K and Feyen L 2017 Global projections of river flood risk in a warmer world *Earth's Future* **5** 171–82

[4] Thober S, Kumar R, Wanders N, Marx A, Pan M, Rakovec O, Samaniego L, Sheffield J, Wood E F and Zink M 2018 Multi-model ensemble projections of European river floods and high flows at 1.5, 2, and 3 degrees global warming *Environ. Res. Lett.* **13** 014003

[5] Clausius R 1850 Über die bewegende kraft der wärme und die gesetze, welche sich daraus für die wärmelehre selbst ableiten lassen *Ann. Phys., Lpz.* **155** 368–97

[6] Levy H, Horowitz L W, Schwarzkopf M D, Ming Y, Golaz J-C, Naik V and Ramaswamy V 2013 The roles of aerosol direct and indirect effects in past and future climate change *J. Geophys. Res.: Atmos.* **118** 4521–32

[7] Samset B H, Sand M, Smith C J, Bauer S E, Forster P M, Fuglestvedt J S, Osprey S and Schleussner C-F 2018 Climate impacts from a removal of anthropogenic aerosol emissions *Geophys. Res. Lett.* **45** 1020–9

[8] Luyssaert S *et al* 2014 Land management and land-cover change have impacts of similar magnitude on surface temperature *Nat. Clim. Change* **4** 389

[9] UNFCCC, editor. Adoption of the Paris Agreement, volume FCCC/CP/2015/L.9/Rev. 1, 2015

[10] Mitchell D *et al* 2017 Half a degree additional warming, prognosis and projected impacts (HAPPI): background and experimental design *Geosci. Model Dev.* **10** 571–83

[11] Sanderson B M *et al* 2017 Community climate simulations to assess avoided impacts in 1.5 and 2 °C futures *Earth Syst. Dyn.* **8** 827–47

[12] Mitchell D, James R, Forster P M, Betts R A, Shiogama H and Allen M 2016 Realizing the impacts of a 1.5 °C warmer world *Nat. Clim. Change* **6** 735–7

[13] Dewan T H 2015 Societal impacts and vulnerability to floods in Bangladesh and Nepal *Weather Clim. Extremes* **7** 36–42

[14] Ghosh S and Dutta S 2012 Impact of climate change on flood characteristics in Brahmaputra basin using a macro-scale distributed hydrological model *J. Earth Syst. Sci.* **121** 637–57

[15] Gain A K, Immerzeel W W, Sperna Weiland F C and Bierkens M F P 2011 Impact of climate change on the stream flow of the lower Brahmaputra: trends in high and low flows based on discharge-weighted ensemble modelling *Hydrol. Earth Syst. Sci.* **15** 1537–45

[16] Alam S, Mostafa Ali M and Islam Z 2016 Future streamflow of Brahmaputra river basin under synthetic climate change scenarios *J. Hydrol. Eng.* **21** 05016027

[17] Pervez M S and Henebry G M 2015 Assessing the impacts of climate and land use and land cover change on the freshwater availability in the Brahmaputra River basin *J. Hydrol.: Reg. Stud.* **3** 285–311

[18] Masood M, Yeh P J-F, Hanasaki N and Takeuchi K 2015 Model study of the impacts of future climate change on the hydrology of Ganges-Brahmaputra-Meghna basin *Hydrol. Earth Syst. Sci.* **19** 747–70

[19] Mirza M M Q, Warrick R A and Ericksen N J 2003 The implications of climate change on floods of the ganges, Brahmaputra and Meghna Rivers in Bangladesh *Clim. Change* **57** 287–318

[20] Mohammed K, Islam A S, Islam G M T, Alfieri L, Bala S K and Khan M J U 2017 Extreme flows and water availability of the brahmaputra river under 1.5 and 2°C global warming scenarios *Clim. Change* **145** 159–75

[21] Betts R A *et al* 2018 Changes in climate extremes, fresh water availability and vulnerability to food insecurity projected at 1.5°C and 2°C global warming with a higher-resolution global climate model *Phil. Trans.* A **376** 20160452

[22] Mohammed K, Islam A K M S, Islam G M T, Alfieri L, Khan M J U, Bala S K and Das M K 2018 Future floods in Bangladesh under 1.5 °C, 2 °C, and 4 °C global warming scenarios *J. Hydrol. Eng.* **23** 04018050

[23] Pendergrass A G, Lehner F, Sanderson B M and Xu Y 2015 Does extreme precipitation intensity depend on the emissions scenario? *Geophys. Res. Lett.* **42** 8767–74

[24] van Oldenborgh G J, Otto F E L, Haustein K and AchutaRao K 2016 The heavy precipitation event of december 2015 in chennai, India [in 'Explaining Extremes of 2015 from a Climate Perspective'] *Bull. Am. Meteorol. Soc.* **97** S87–91

[25] Bellouin N, Rae J, Jones A, Johnson C, Haywood J and Boucher O 2011 Aerosol forcing in the Climate Model Intercomparison Project (CMIP5) simulations by HadGEM2-ES and the role of ammonium nitrate *J. Geophys. Res.: Atmos.* **116** D20206

[26] Donlon C J, Martin M, Stark J, Roberts-Jones J, Fiedler E and Wimmer W 2012 The Operational Sea Surface Temperature and Sea Ice Analysis (OSTIA) system *Remote Sens. Environ.* **116** 140–58

[27] Taylor K E, Stouffer R L and Meehl G A 2012 An overview of CMIP5 and the experiment design *Bull. Amer. Meteor. Soc.* **93** 485–98

[28] Kay J E *et al* 2015 The Community Earth System Model (CESM) Large ensemble project: a community resource for studying climate change in the presence of internal climate variability *Bull. Am. Meteorol. Soc.* **96** 1333–49

[29] Lehner B and Grill G 2013 Global river hydrography and network routing: baseline data and new approaches to study the world's large river systems *Hydrol. Process.* **27** 2171–86 (www.hydrosheds.org).

[30] Karl T R, Nicholls N and Ghazi A 1999 *CLIVAR/GCOS/WMO Workshop on Indices and Indicators for Climate Extremes Workshop Summary* (Dordrecht: Springer Netherlands) pp 3–7

[31] Sillmann J, Kharin V V, Zhang X, Zwiers F W and Bronaugh D 2013 Climate extremes indices in the CMIP5 multimodel ensemble: Part 1. Model evaluation in the present climate *J. Geophys. Res.: Atmos.* **118** 1716–33

[32] Ménégoz M, Gallée H and Jacobi H W 2013 Precipitation and snow cover in the Himalaya: from reanalysis to regional climate simulations *Hydrol. Earth Syst. Sci.* **17** 3921–36

[33] Immerzeel W W, Wanders N, Lutz A F, Shea J M and Bierkens M F P 2015 Reconciling high-altitude precipitation in the upper indus basin with glacier mass balances and runoff *Hydrol. Earth Syst. Sci.* **19** 4673–87

[34] Cannon A J, Sobie S R and Murdock T Q 2015 Bias correction of gcm precipitation by quantile mapping: How well do methods preserve changes in quantiles and extremes? *J. Clim.* **28** 6938–59

[35] Chevuturi A, Klingaman N P, Turner A G and Hannah S 2018 Projected changes in the asian-australian monsoon region in 1.5°C and 2.0°C global-warming scenarios *Earth's Future* **145** 159–75

[36] Lee D, Min S-K, Fischer E, Shiogama H, Bethke I, Lierhammer L and Scinocca J F 2018 Impacts of half a degree additional warming on the asian summer monsoon rainfall characteristics *Environ. Res. Lett.* **13** 044033

[37] Saeed F, Bethke I, Fischer E, Legutke S, Shiogama H, Stone D A and Schleussner C-F 2018 Robust changes in tropical rainy season length at 1.5°C and 2°C *Environ. Res. Lett.* **13** 064024

[38] Sampson C C, Smith A M, Bates P D, Neal J C, Alfieri L and Freer J E 2015 A high-resolution global flood hazard model *Water Resour. Res.* **51** 7358–81

[39] Bates P D, Horritt M S and Fewtrell T J 2010 A simple inertial formulation of the shallow water equations for efficient two-dimensional flood inundation modelling *J. Hydrol.* **387** 33–45

[40] Yamazaki D, Ikeshima D, Tawatari R, Yamaguchi T, O'Loughlin F, Neal J C, Sampson C C, Kanae S and Bates P D 2017 A high-accuracy map of global terrain elevations *Geophys. Res. Lett.* **44** 5844–53

[41] Smith A, Sampson C and Bates P 2015 Regional flood frequency analysis at the global scale *Water Resour. Res.* **51** 539–53

[42] Wing O E J, Bates P D, Sampson C C, Smith A M, Johnson K A and Erickson T A 2017 Validation of a 30 m resolution flood hazard model of the conterminous united states *Water Resour. Res.* **53** 7968–86
[43] Aljazeera 2017 Floods kill over 1,200 in India, Nepal and Bangladesh (http://aljazeera.com/news/2017/08/floods-kill-1200-india-nepal-bangladesh-170826230610924.html) (Accessed: 23 October 2017)
[44] The Guardian 2017 While the world's attention is elsewhere, Bangladesh faces a humanitarian crisis (https://theguardian.com/voluntary-sector-network/2017/sep/12/bangladesh-severe-disaster-flooding) (Accessed: 23 October 2017)
[45] Floodlist 2017 Bangladesh—Rivers at Record High, Floods Affect 1.3 Million (http://floodlist.com/asia/bangladesh-floods-august-2017) (Accessed: 20 October 2017)
[46] Pekel J-F, Cottam A, Gorelick N and Belward A S 2016 High-resolution mapping of global surface water and its long-term changes *Nature* **540** 418
[47] Fischer E M, Beyerle U, Schleussner C F, King A D and Knutti R 2018 Biased Estimates of Changes in Climate Extremes From Prescribed SST Simulations. *Geophys. Lett.* **45** 8500–09
[48] He J and Soden B J 2016 The impact of SST biases on projections of anthropogenic climate change: A greater role for atmosphere-only models? *Geophys. Res. Lett.* **43** 7745–50
[49] Lutz A F, Immerzeel W W, Shrestha A B and Bierkens M F P 2014 Consistent increase in high Asia's runoff due to increasing glacier melt and precipitation *Nat. Clim. Change* **4** 587
[50] Kraaijenbrink P D A, Bierkens M F P, Lutz A F and Immerzeel W W 2017 Impact of a global temperature rise of 1.5 degrees Celsius on Asia's glaciers *Nature* **549** 257
[51] Immerzeel W W, Pellicciotti F and Bierkens M F P 2013 Rising river flows throughout the twenty-first century in two Himalayan glacierized watersheds *Nat. Geosci.* **6** 742
[52] Shea J M and Immerzeel W W 2016 An assessment of basin-scale glaciological and hydrological sensitivities in the Hindu Kush-Himalaya *Ann. Glaciol.* **57** 308–18